

# Micromachined p-GaN Gate Normally-off Power HEMT with an Optimized Air-bridge Matrix Layout Design

Chih-Wei Yang, Hsiang-Chun Wang, Hsien-Chin Chiu,  
Chien-Kai Tung\*, Tsung-Cheng Chang\* and Schang-jing Hon\*

Department of Electronics Engineering, Chang Gung University, Taiwan, R.O.C.  
Email: [hcchiu@mail.cgu.edu.tw](mailto:hcchiu@mail.cgu.edu.tw) TEL: +886-3-2118800 # 3645

**KEYWORDS: P-GaN, HEMT, Normally-off, ABM, Micromachined**

## Abstract

In this work, a micromachined P-GaN power high electron mobility transistor (HEMT) on Si substrate with new air-bridged matrix design was demonstrated. After removal of the Si substrate beneath the P-GaN HEMT, a significant breakdown voltage improvement was observed. The drain and source terminals were arranged as the matrix type and the 3  $\mu\text{m}$ -thick Au was adopted for terminals connection and current redistribution layer of the proposed power cell. Compared with the traditional multi-fingers layout, the current density was improved.

## INTRODUCTION

Recently, GaN on Si (111) technology has been widely demonstrated for electronic devices due to its low cost and the superior scalability of the wafer [1]. However, GaN devices that are fabricated on Si substrate have the disadvantage that electrical breakdown occurs vertically through the silicon substrate, because of the large lattice mismatch between the GaN and the Si and the comparatively low Si electrical field strength (0.3 MV/cm). Furthermore, another significant epitaxial problem arises from the large thermal expansion coefficient mismatch between GaN and Si substrate [2]. These difficulties result in the serious wafer bending strain and residual stress after Si substrate thinning process for final package. In this paper, a micromachined HEMT with air-bridged matrix (M-ABM) redistribution layer design is proposed.

## DEVICE FABRICATION

Fig.1 shows the cross-section of P-GaN HEMT with backside micromachined. The device with a 2  $\mu\text{m}$  gate length which was on top of 4  $\mu\text{m}$  length P-GaN layer, the gate-to-source and gate-to-drain distance were 6  $\mu\text{m}$  and 20  $\mu\text{m}$ , respectively. After the completion of the front-side fabrication, the Si substrate was thinned down to 100  $\mu\text{m}$ . Then the Si substrate beneath the active region was removed by  $\text{SF}_6$  plasma etching, until the N-face buffer layer was exposed. For reducing the substrate leakage current and enhancing the thermal management, the  $\text{SiO}_2/\text{Cu}$  (100 nm/20  $\mu\text{m}$ ) were deposited on the backside of the 4 inch wafer. In order to compare the device characteristics, the standard power device with parallel drain/source multi-fingers (MF) design which shown in

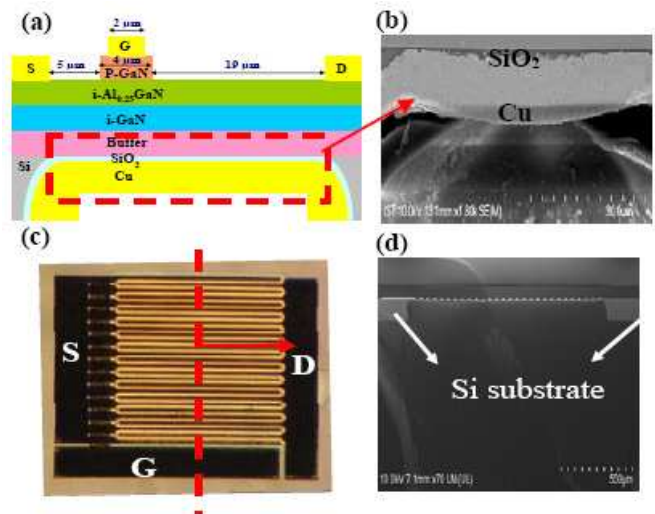


Fig.1(a) Cross-section of P-GaN HEMT with backside micromachined. (b) SEM image of backside micromachined. (c) Top-view of multi-finger P-GaN HEMT. (device size = 1.34  $\times$  1.34 mm<sup>2</sup>) (d) SEM image of multi-finger P-GaN HEMT with backside micromachined.

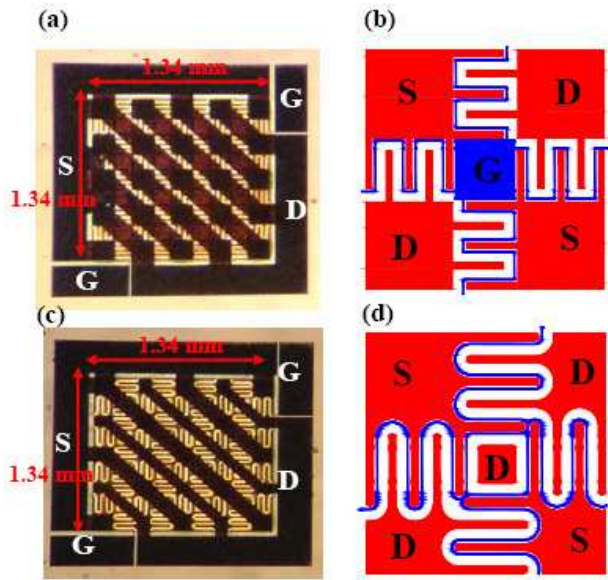


Fig.2(a) Top-view of ABM P-GaN HEMT (device size =  $1.34 \times 1.34 \text{ mm}^2$ ) (b) ABM Layout of a  $2 \times 2$  matrix cell. (c) Top-view of new ABM P-GaN HEMT. (device size =  $1.34 \times 1.34 \text{ mm}^2$ ) (d) New ABM Layout of a  $2 \times 2$  matrix cell.

Fig. 1(c) and 1(d) were fabricated on the same wafer and the device size was  $1.34 \times 1.34 \text{ mm}^2$ . Figure 2(a) and 2(b) exhibited the previous design called air-bridge matrix (ABM), and the new ABM design was shown in Fig 2(c) and 2(d). For comparison, size of both devices is  $1.34 \times 1.34 \text{ mm}^2$ .

### MEASUREMENT RESULTS AND DISCUSSIONS

Fig. 3 displays  $I_{DS}-V_{GS}$  and  $g_m-V_{GS}$  characteristics of MF, ABM and new ABM P-GaN HEMT with backside micromachined at  $V_{DS} = 5 \text{ V}$ , respectively. An obvious current improvement is observed for ABM and new ABM P-GaN HEMT due to the air-bridge matrix structure increasing the current density from one-dimension to two-dimensions. As shown in Fig 3, threshold voltages ( $V_{th}$ ) of three devices were  $+0.7 \text{ V}$ ; the  $I_{DS}$  is  $1.55 \text{ A}$  of MF P-GaN HEMT and it can be improved to  $2.28 \text{ A}$  by using the new ABM design, it is about 47 % current improvement. Fig. 4 presents the  $I_{DS}-V_{DS}$  characteristic of three HEMTs with backside micromachined at  $V_{GS}$  from 4 to 0 V. The  $R_{DS,on}$  was extracted at  $V_{GS} = 4 \text{ V}$ ; and it is  $2.25 \Omega$  for MF P-GaN HEMT,  $1.9 \Omega$  for ABM P-GaN HEMT and  $1.64 \Omega$  for new ABM P-GaN HEMT, respectively. The smaller  $R_{DS,on}$  for new ABM P-GaN HEMT was ascribed to improve the current density, increase the total gate

width and reduce the transmission distance between drain and source region. In addition, the current flow of MF-HEMT is one-dimension, and the current crowding occurs at the drain electrode due to high electric field. However, the current flows of ABM and new ABM design were two-dimension, therefore the current can be distributed and current crowding can be weakened. The three-terminal off-state breakdown voltages ( $V_{BR}$ ) of three HEMTs measured using an Agilent B1505A measurement system is shown in Fig. 5. In this work,  $V_{BR}$  is defined as the voltage at which a drain leakage current between the drain and the source terminals reaches  $1 \text{ mA}$  at a  $V_{GS}$  of  $0 \text{ V}$ . The drain leakage current of MF P-GaN HEMT increases rapidly following an increase of  $V_{DS}$  and its  $V_{BR}$  is  $188 \text{ V}$ . This value can be improved to  $274 \text{ V}$  with the new ABM

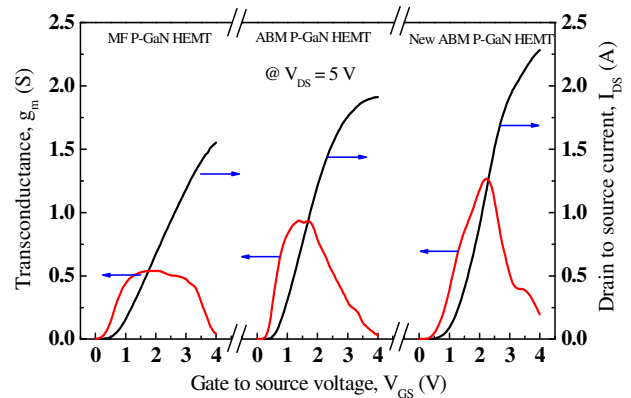


Fig.3  $I_{DS}-V_{GS}$  and  $g_m-V_{GS}$  characteristic of MF, ABM and new ABM P-GaN HEMT with backside micromachined at  $V_{DS} = 5 \text{ V}$ .

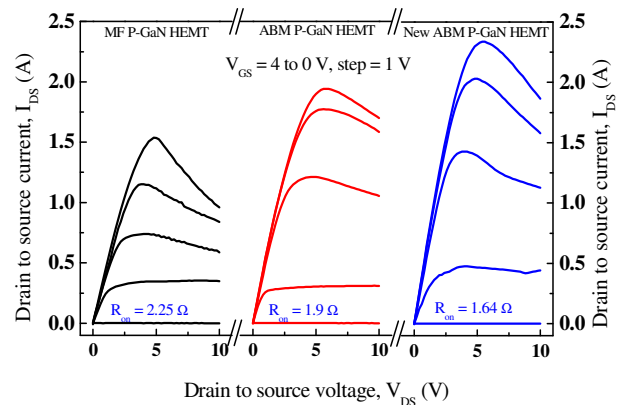


Fig. 4  $I_{DS}-V_{DS}$  characteristics of MF, ABM and new ABM P-GaN HEMT with backside micromachined.

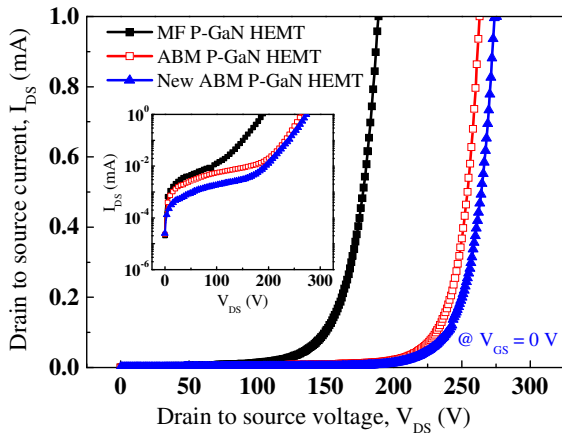


Fig.5 Three-terminal off-state breakdown voltage measurements for MF, ABM and new ABM P-GaN HEMT with backside micromachined at  $V_{GS} = 0$  V.

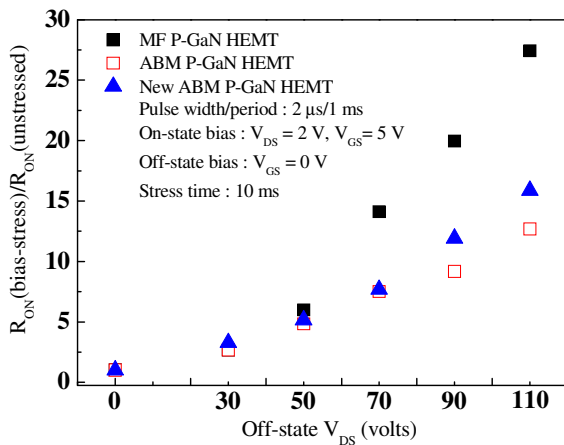


Fig.6 Dynamic  $R_{on}$  measurement for MF, ABM and new ABM P-GaN HEMT with backside micromachined.

design, due to the mesa sidewall leakage path which eliminated by the air-bridged structure. Fig. 6 shows the dynamic  $R_{on}$  measurement, which was measured by utilizing an Agilent 1267A measurement system. Devices were biased at on-state ( $V_{GS} = 5$  V and  $V_{DS} = 2$  V) and off-state ( $V_{GS} = 0$  V,  $V_{DS} = 0$  to 110 V). An obvious increase of  $R_{on}$  was obtained from MF P-GaN HEMT with an increase of  $V_{DS}$ . On the other hand, ABM P-GaN HEMT shows a slighter increase of  $R_{on}$  than the new ABM one. It is believed that the drift regions of new ABM design is larger than ABM design and caused higher surface traps and made the higher increase of  $R_{on}$ .

## CONCLUSION

This paper demonstrates a micromachined-ABM that improves the  $V_{BR}$  and dynamic  $R_{on}$  of P-GaN HEMTs. Removing the Si substrate and using a  $SiO_2/Cu$  thermal sinking layer improve the  $V_{BR}$  from 188 V to 274 V. The current density was also improved by using the new ABM design due to reduce the channel thermal accumulation.

## REFERENCES

- [1] K. Cheng, M. Leys, S. Degroote, "AlGaIn/GaN high electron mobility transistors grown on 150 mm Si (111) substrates with high uniformity," *Jpn. J. Appl. Phys.*, vol. 47, no. 3, pp. 1553–1555, Mar. 2008.
- [2] S. Raghavan and J. Redwing, "Growth stresses and cracking in GaN films on (111) Si grown by metalorganic chemical vapor deposition. II. Graded AlGaIn buffer layers," *J. Appl. Phys.*, vol. 98, no. 2, pp. 023515-1–023515-3, 2005.

## ACRONYMS

- HEMT High Electron Mobility Transistor  
 ABM Air-Bridge Matrix

